

Preparation and characterization of Sr Substituted $\text{BaBi}_2\text{Nb}_2\text{O}_9$ Ceramics

A THESIS SUBMITTED IN PARTIAL FULFILLMENT OF
THE REQUIREMENTS FOR THE DEGREE OF
BACHELOR OF TECHNOLOGY

By

PRASHANTA KUMAR PRADHAN

Roll no:- 109CR0013



**DEPARTMENT OF CERAMIC ENGINEERING
NATIONAL INSTITUTE OF TECHNOLOGY
ROURKELA**

2012-2013

Preparation and characterization of Sr Substituted $\text{BaBi}_2\text{Nb}_2\text{O}_9$ Ceramics

A THESIS SUBMITTED IN PARTIAL FULFILLMENT OF
THE REQUIREMENTS FOR THE DEGREE OF
BACHELOR OF TECHNOLOGY

By

PRASHANTA KUMAR PRADHAN

Roll no:- 109CR0013

UNDER THE GUIDANCE OF

DR. JAPES BERA



**DEPARTMENT OF CERAMIC ENGINEERING
NATIONAL INSTITUTE OF TECHNOLOGY
ROURKELA**

2012-2013



NATIONAL INSTITUTE OF TECHNOLOGY ROURKELA

CERTIFICATE

This is to certify that the thesis entitled, “Preparation and characterization of Sr Substituted $\text{BaBi}_2\text{Nb}_2\text{O}_9$ Ceramics ” submitted by *PRASHANTA KUMAR PRADHAN* in partial fulfilment of the requirements of the award of Bachelor of Technology Degree in Ceramic Engineering at National Institute Of Technology, Rourkela is an authentic work carried out by him under my supervision and guidance.

To the best of my knowledge, the matter embodied in the thesis has not been submitted to any other university / institute for the award of any Degree or Diploma.

Date:

Dr. Japes Bera
(Associate Professor)
Dept. of Ceramic Engineering
National Institute of Technology
Rourkela-769008

Acknowledgement

I wish to express my deep sense of respect and regard for Prof. Japes Bera, Department of Ceramic Engineering, N.I.T Rourkela for introducing the research topic and for his inspiring guidance, constructive criticism and valuable suggestions throughout this research work. I would also like to thank him for his constant support and words of encouragement without which it would not have been possible for me to complete this research work.

I am also grateful to all the faculty members of the Dept. of Ceramic Engineering, whose immense knowledge in the field of ceramics has enlightened me in various areas of my research work.

I am also grateful to Mr Ganesh Kumar Sahoo, Miss Geetanjali Parida and all the other research scholars in the Dept. of Ceramic Engineering for their unparalleled help and support.

I am also thankful to Mr Prashant Mohanty, Mr Sushil Sahoo and all the other office staff for all their help. I would also like to thank my friends for all their suggestions and inputs for the betterment of my research work.

Finally, I deeply thank my parents for all their support and faith in me.

PRASHANTA KUMAR PRADHAN

Roll no:- 109CR0013

**B.Tech, Dept. of Ceramic Engineering
N.I.T Rourkela**

:CONTENTS:

<i>TITLE</i>	<i>PAGE NO.</i>
<i>Acknowledgement</i>	<u>04</u>
<i>List of Figures</i>	<u>07</u>
<i>List of Tables</i>	<u>07</u>
<i>Abstract</i>	<u>08</u>
<i>Chapter 1- Introduction</i>	<u>09</u>
<i>Chapter 2 -Literature review</i>	<u>13</u>
<i>2.1 Introduction</i>	<u>14</u>
<i>2.2 Summary of the literature review</i>	<u>15</u>
<i>Chapter 3- Experimental procedure</i>	<u>16</u>
3.1: Introduction	<u>17</u>
3.2:Batch calculation	<u>17</u>
3.3: Pallet fabrication process	<u>17</u>
3.4 : Characterization of sample	<u>20</u>
3.4.1 Density measurements	<u>20</u>
3.4.2 Microstructural study	<u>20</u>
3.4.3 Phase analysis	<u>21</u>
3.4.4 Electrical properties measurement.	<u>22</u>
3.4.4.1 Dielectric properties measurement	<u>22</u>
3.4.4.2 Polarization with electric field study.	<u>23</u>
<i>Chapter 4 -Results and discussions</i>	<u>24</u>
4.1: Density measurement	<u>25</u>

4.2 : Phase formation behaviour	<u>26</u>
4.3 Microstructural analysis	<u>29</u>
4.4 : Electrical properties analysis	<u>31</u>
<i>Chapter 5- Conclusion</i>	<u>34</u>
<i>Chapter 6 -References</i>	<u>36</u>

List of Figures

Figure number	Figure caption	Page No.
1	Typical structure of $\text{Bi}_4\text{Ti}_3\text{O}_{12}$ ($n = 3$) BLSFs	11
2	Flow chart of materials synthesis by solid oxide route method.	19
3	The XRD pattern of samples sintered at 1100°C for a holding time of 4 hours.	27
4	Lattice parameter values comparison of SBN^{*1} , BBN^{*2} and their 1:1 solid solutions.	28
5	Figure (a) Micro structure of pure BBN	39
	Figure 5(b) Micro structure of pure SBN	39
	Figure 5(c) Micro structure of 25% SBN-75%BBN	30
	Figure 5(d)Micro structure of 50% SBN-50% BBN	30
	Figure 5(e)Micro structure of 75% SBN-25%BBN	31
6	Permittivity vs frequency plot	32
7	Frequency vs loss factor plot	32
8	Polarisation vs electric field plot	33

*1= $\text{SrBi}_2\text{Nb}_2\text{O}_9$, *2= $\text{BaBi}_2\text{Nb}_2\text{O}_9$

List of Tables

Table number	Table caption	Page No.
1	List of compositions to be prepared	17
2	Amount of batch calculated raw materials required for the preparation of sample of 5 gm each	18
3	Comparison of AP and BD values of pallets sintered at 1050°C for batch 1	25
4	Comparison of AP and BD values of pallets sintered at 1100°C for batch 2	25
5	Comparison of AP and BD values of pallets sintered at 1100°C for batch 3	26

ABSTRACT

BaBi₂Nb₂O₉, SrBi₂Nb₂O₉ and their solid solution composition powder were synthesized by solid state reaction route. The 2 layer BLSF compounds and solid solution phases were developed at a calcination temperature of 900⁰c. The powders were uniaxially pressed into pellets and were sintered at a sintering temperature of 1100⁰c. The densified ceramic shows an anisotropic grain structure which was investigated using scanning electron microscope. BLSF phase formation was confirmed by XRD analysis. Dielectric and ferroelectric properties measurement, silver electrode were applied on both surfaces of the pellets. Electrical properties were measured using Hioki LCR meter. The ferroelectric polarization of the materials was measured in a loop tracer. The dielectric and ferroelectric properties of solid solution compositions were better than individual pure composition.

CHAPTER 1

INTRODUCTION

Introduction

Bismuth layered structure ferroelectrics (BLSF) compounds are of great technological interest in modern microelectronic applications. Aurivillius and Subbarao first reported the synthesis and ferroelectricity of these compounds [1-3]. They are proposed [4-6] for applications in Ferroelectric Random Access Memory (FeRAM) and Dynamic Random Access Memories (DRAM). They have advantages of high Curie temperature (T_c), low temperature coefficient of dielectrics, low ageing rate and strong anisotropic characteristics and lead-free composition [7, 8]. Due to their higher Curie temperature and lead free composition they have been proposed for several piezoelectric applications [9].

The general crystal structure of BLSF is $\text{Bi}_2\text{A}_{m-1}\text{B}_m\text{O}_{3m+3}$, where A is the combination of mono, di or tri-valent cations at 12-coordinated site; B is a combination of ions for octahedrally coordinated sites which may be tetra, penta and hexa valent ions with smaller ionic radius and m corresponds to the number of BO_6 octahedral layers ($m=1, 2, 3, 4$, and 5) in pseudo perovskite blocks interleaved between the $(\text{Bi}_2\text{O}_2)^{2+}$ layer. The schematic structure of BLSF is shown in Fig. 1.

A typical 3-layer ($m=3$) BLSF compound $\text{Bi}_4\text{Ti}_3\text{O}_{12}$ (BIT) has been widely investigated because of its low switching field and high Curie temperature (670°C). The spontaneous polarization (P_s) of BLSFs arises along a axis due to the displacement of Bi ion. However, odd member of m , such as BIT shows a small P_s along the c -axis together with large P_s along a -axis. The BLSF with even number of m such as $\text{SrBi}_4\text{Ti}_4\text{O}_{15}$ (SBTi) with $m=4$, shows no polarization along c -axis because of mirror symmetry of their orthorhombic crystal structure. Although the BIT has large P_s compared to SBTi, it suffers from poor insulating properties. In

contrast SBTi has sufficiently high insulating properties. Continuous efforts have been made to improve the electrical properties of these BLSFs.

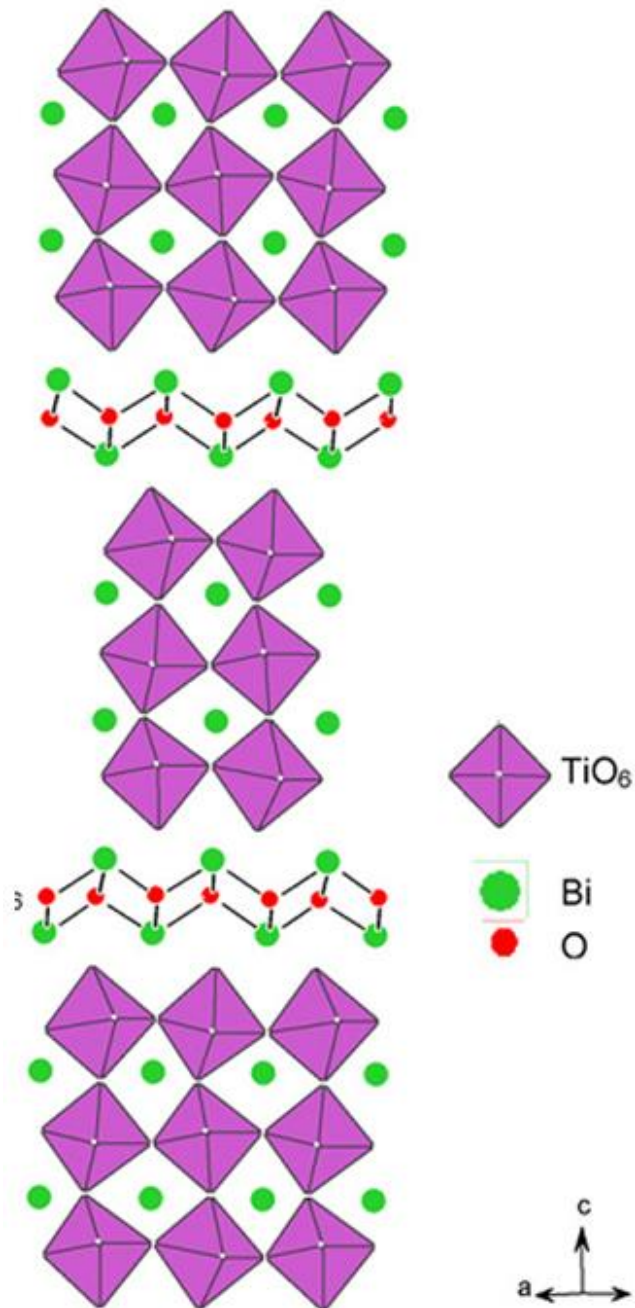


Fig.1. Typical structure of $\text{Bi}_4\text{Ti}_3\text{O}_{12}$ ($n=3$) BLSFs

Among BLSF compounds, most of them possess normal ferroelectric behaviour while only a few such as $\text{BaBi}_2\text{Nb}_2\text{O}_9$, $\text{BaBi}_2\text{Ta}_2\text{O}_9$, $\text{BaBi}_4\text{Ti}_4\text{O}_{15}$ exhibit relaxor behaviour. Ferroelectric relaxors are used for multiple applications owing to their exceptional dielectric properties. They can be applied in multilayer ceramic capacitors, electro-optic devices, ultrasonic and medical imaging devices.

The $\text{BaBi}_2\text{Nb}_2\text{O}_9$ (BBN) relaxor seems to be promising for future capacitor application from the point of environmental friendly lead-free relaxor material. $\text{SrBi}_2\text{Nb}_2\text{O}_9$ (SBN) is interesting due to its excellent fatigue free behaviour and low leakage current. It has also high Curie temperature. The SBN material has been investigated as piezoelectric materials for resonator and filter application because of their low temperature coefficient of resonator frequency.

In the BLSF structure A site can accommodate many +2 cations like Sr^{2+} , Ba^{2+} and b sites can accommodate many +4 and +5 cations like Ti^{2+} , Nb^{5+} , V^{5+} and they have many possibilities of modifying their ferroelectric properties by this A and /or B site substitutions. A great effort has been given to investigate the substitution effect on the ferroelectric properties of BLSF compound. Here the substitution of Sr in place of Ba in BBN ceramics will be also a promising for enhancement of dielectric and ferroelectric properties of BBN – SBN ceramics.

CHAPTER 2

LITERATURE REVIEW

2.1 Introduction

In this section a summary of all the literature on the topic of $\text{BaBi}_2\text{Nb}_2\text{O}_9$ and $\text{SrBi}_2\text{Nb}_2\text{O}_9$ will be describe and the change in the behaviour with different dopant concentration also be discussed with the various preparation method of the materials..

Co-precipitation method for the preparation of fine ferroelectric $\text{BaBi}_2\text{Nb}_2\text{O}_9$ was studied by S.P. Gaikwada, H.S. Potdara, Violet Samuel, V. Ravi on 2005 [10]. It concluded from this paper that A simple co-precipitation technique is described for the preparation of fine powders of $\text{BaBi}_2\text{Nb}_2\text{O}_9$. The BBN phase was found to be formed on calcining the precipitate at 800°C with average particle size of 100 nm. The dielectric and ferroelectric properties of BBN prepared by this process are also reported.

The Dielectric and AC conductivity behavior of $\text{BaBi}_2\text{Nb}_2\text{O}_9$ ceramics was examined by C. Karthik, and K.B.R. Varma.[11] the dielectric constant at various temperatures and the frequency dependence of conductivity confirms the relaxor behavior of the ceramics.

Influence of vanadium dopant on relaxor behavior of $\text{BaBi}_2\text{Nb}_2\text{O}_9$ ceramics was explained by M. Adamczyk, L.Kozielska, M.Pilch, M.Pawczyk, A.Soszyn'. [12] The mixture of vanadium ions to BBN ceramics has an influence on the shape and size of grains.

A lot of experiments have also done with the SBN ceramics.

Effect of V^{+5} doping on Structural and Dielectric properties of $\text{SrBi}_2\text{Nb}_2\text{O}_9$ prepared at low temperature was studied by Puja Goel, K.L. Yadav on 2006[13]. It is summarized that V^{+5} doping in layer-structured SBN ceramics has an significant influence on dielectric and electric properties upto 15% doping. in the 100 Hz–100 KHz frequency range at various temperatures vanadium doped SBN ceramic has shown strong low frequency dielectric dispersion

Influence of Sm_2O_3 doping on formation and structure of $\text{SrBi}_2\text{Nb}_2\text{O}_9$ nanocrystals in lithium borate glasses was reported by B. Harihara Venkataramana, T. Fujiwarab, K.B.R. Varma, T. Komatsua [5]. The conclusion found here that New glasses of $16.66\text{SrO}-16.66[(1-x)\text{Bi}_2\text{O}_3-x\text{Sm}_2\text{O}_3]-16.66\text{Nb}_2\text{O}_5-50\text{Li}_2\text{B}_4\text{O}_7$ were prepared and their initial crystallization behaviors were examined. It was found from XRD analyses, TEM observations, and Raman scattering spectrum measurements that the initial crystalline phase formed in these glasses has been fluorite-type SBN nano crystals and Sm^{3+} ions are incorporated into fluorite-type SBN nano crystals.

Structure and electrical properties of bismuth and sodium modified $\text{SrBi}_2\text{Nb}_2\text{O}_9$ ferroelectric ceramics was studied by Pinyang Fang, Huiqing Fan, Zengzhe Xi, Weixing Chen a, Shanchuan Chen, Wei Long, Xiaojuan in the year 2013[14]. The conclusion got from the experiments was that the piezoelectric coefficient and Curie temperature of the SBNBN_4 specimen were found to be 22 pC/N and $586.5\text{ }^\circ\text{C}$, respectively. Also the temperature stability of piezoelectric properties for SBN specimen was significantly enhanced by the (Bi, Na) ions modification.

2.2 Summary of the literature review:

From the literature review it is found that there has not any study exist about the Sr doped $\text{BaBi}_2\text{Nb}_2\text{O}_9$ ceramics. So this provide a wide scope of working in this project of preparation and characterization of Sr Substituted $\text{BaBi}_2\text{Nb}_2\text{O}_9$.

Chapter 3

Experiments

Experimental

3.1 Introduction

BaBi₂Nb₂O₉ (BBN) and **SrBi₂Nb₂O₉ (SBN)** and there solid solutions were synthesized by solid oxide route method. The conventional solid state route uses simple processing steps and relatively less costly raw materials. However, the temperature requirement for the formation of pure phase powder and its densification is quite high. The materials contained in the Table .1 were synthesized and their properties were studied.

Table 1.List of compositions to be prepared

BaBi ₂ Nb ₂ O ₉ (pure)
BaBi ₂ Nb ₂ O ₉ (25%)- SrBi ₂ Nb ₂ O ₉ (75%)
BaBi ₂ Nb ₂ O ₉ (50%)- SrBi ₂ Nb ₂ O ₉ (50%)
BaBi ₂ Nb ₂ O ₉ (75%)- SrBi ₂ Nb ₂ O ₉ (25%)
SrBi ₂ Nb ₂ O ₉ (pure)

3.2 Batch calculation

Table 2 below depict the required calculated raw materials with their quantities for the preparation of the respective compositions.

3.3 Procedure for the preparation of the pallets

For the preparation of the pallets of our desired composition materials mention on the Table 2 with their calculated amount of raw materials oxides was weighed using an clean water paper. Then the batches were mixed in an agate mortar and grinded for about 1 hour. For the ease

of the grinding process continuously acetone was added to the mixture. Then all the well mixed batches of were taken in a clean alumina crucible and calcined in an oven at a temperature of 800⁰C for a holding time of 4 hours. After the cooling of the oven the materials were taken out and few drops of 3 wt % Polyvinyl Alcohol (PVA) was added to it as a binder for granulation. After that powders were taken in a clean mould of 13 mm die size and pressed at a pressure of 4.5 N/ms²area. Now the green pallets were ready to sinter.

Table 2 Amount of batch calculated raw materials required for the preparation of sample of 5 gm each

Sample name	Raw materials	Quantities(in grams)
BaBi ₂ Nb ₂ O ₉ (pure)	BaCo ₃	1.114
	Bi ₂ O ₃	2.632
	Nb ₂ O ₉	1.5
BaBi ₂ Nb ₂ O ₉ (75%)- SrBi ₂ Nb ₂ O ₉ (25%)	BaCo ₃	0.8288
	Bi ₂ O ₃	2.632
	Nb ₂ O ₉	1.502
	SrCo ₃	0.20
BaBi ₂ Nb ₂ O ₉ (50%)- SrBi ₂ Nb ₂ O ₉ (50%)	BaCo ₃	0.5682
	Bi ₂ O ₃	2.683
	Nb ₂ O ₉	1.531
	SrCo ₃	0.425
BaBi ₂ Nb ₂ O ₉ (25%)- SrBi ₂ Nb ₂ O ₉ (75%)	BaCo ₃	0.2761
	Bi ₂ O ₃	2.722
	Nb ₂ O ₉	1.542
	SrCo ₃	0.6468
SrBi ₂ Nb ₂ O ₉ (pure)	SrCo ₃	0.875
	Bi ₂ O ₃	2.624
	Nb ₂ O ₉	1.46

Now one pallet from each batch was fired in a pit furnace at different temperatures. Very good densities of the pallets were found at a sintering temperature of 1100⁰C.

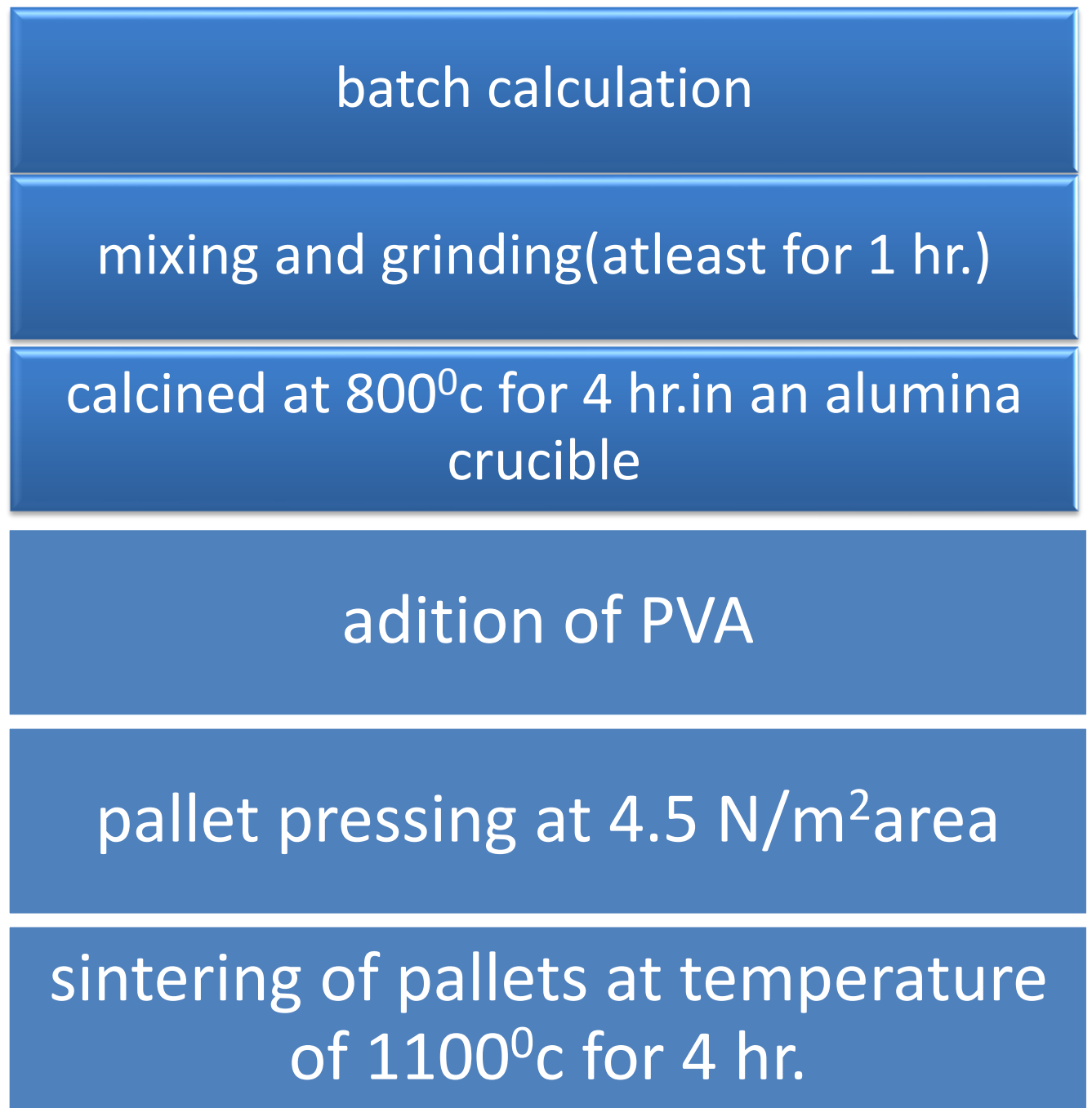


Figure 2. Flow chart of materials synthesis by solid oxide route method.

3.4 Characterization of samples

3.4.1 Density measurements

Densities of sintered samples were measured effectively by Archimedes principle. The basic procedure was as follows. The dry weight of the sintered samples was measured. The sintered samples were then immersed in water and kept under a vacuum of 4 mm of mercury for 2hrs. this process was continued till the bubbles were ejecting from the samples. The suspended weight of the pellet was then measured in water and then the soaked weight was measured by washing the pellet with a wet paper towel. The apparent porosity and bulk densities were calculated as follows:

$$\% P_{App} = \frac{W_s - W_d}{W_s - W_a} \times 100 \quad (3.1)$$

$$D_{bulk} = \frac{W_d}{W_s - W_a} \quad (3.2)$$

where, W_s = Soaked weight of the sample, W_d = Dry weight of the sample, W_a = Suspended weight of the sample.

3.4.2 Microstructural study

A scanning electron microscope (SEM) is a type of electron microscope that produces images of a sample by scanning it with a focused beam of electrons. The electrons interact with electrons in the sample, producing various signals that can be detected and that contain information about the sample's surface topography and composition. The electron beam is generally scanned in a raster scan pattern, and the beam's position is combined with the detected

signal to produce an image. SEM can achieve resolution better than 1 nanometer. Specimens can be observed in high vacuum, low vacuum and in environmental SEM specimens can be observed in wet conditions. The samples were scan by SEM with a silver coating over it and there grains were studied.

3.4.3 Phase analysis

X-ray diffraction is a very powerful tool for material characterization. Various physical properties such as optical, magnetic, ferroelectric, electric, etc. depend on their chemical composition and the atomic arrangement of the specimen. X-ray diffraction pattern provides important information such as: (i) qualitative phase composition of the sample, (ii) intensities of diffraction peaks providing quantitative information of the phases, (iii) inter-planar spacing of different phases, (iv) unit cell parameters and lattice type of different phases, (v) crystallite size of phases, and (vi) stress and strain present in the lattice.

Phase formation of calcined and sintered powder samples was studied by powder X-ray diffraction, performed with a Philip's Diffractometer (Model: PW-1830, Philips, Netherlands). The source is Cu K α having a wavelength of 1.541874 Å and equipped with Ni β -filter. To detect the diffracted X-rays; an electronic detector is placed on the other side of the sample from the ray tube and the sample was rotated through different Bragg's angles. The goniometer keeps track of the angle 2θ and the detector records the diffracted X-rays in units of counts/sec and transmit this information to the computer. To carry out the XRD the parameter set were , scanning range of 20° - 60° and a step size of $1.5^{\circ}/\text{min}$. The diffraction pattern of the sample was plotted as X-ray intensity (counts/sec) against the angle 2θ . The 2θ for each diffraction peak was converted to d -spacing, using the Bragg's law that is $n\lambda = 2d \sin\theta$, where λ is the wave length of X-ray and n is order of diffraction.

Identification of the different phases present was carried out by Hanawalt method using Philips X-pert Highscore software. The samples pattern comprises of a set of peak positions “ 2θ ” and a set of relative peak intensities I . But the angular position of the peaks depends on the wavelength used and a more fundamental quantity is the spacing d of the lattice planes forming each peak. Each pattern is described by listing the d and I values of its diffraction peaks. Each substance is characterized by d values of its 3 strongest peaks. The d values together with the relative intensities are sufficient to characterize the pattern of an unknown phase

Lattice parameters were determined by using the following relationship for orthorhombic structure .

$$\frac{1}{d^2} = \frac{h^2}{a^2} + \frac{k^2}{b^2} + \frac{l^2}{c^2} \quad (3.3)$$

where, a , b and c are the lattice parameters, d is the interplanar spacing and (hkl) are Miller indices.

3.4.4 Electrical properties measurement.

3.4.4.1 Dielectric properties measurement

A dielectric is an electrical insulator that can be polarized by an external electric field. When a dielectric material is placed in an electric field, electric charges do not flow through the material as they do in a conductor, but only slightly shifting from their average equilibrium positions occurs and causes a dielectric polarization. Because of the dielectric polarization, positive charges are displaced toward the field and negative charges shift in the opposite direction. This results in an internal electric field which reduces the overall field within the dielectric itself. If a dielectric is composed of weakly bonded molecules, those molecules not only become polarized, but also reorient themselves so that their symmetry axis aligns to the field.

The capacitance (C) of a dielectric capacitor is given by the following formula,

$$C = \frac{\epsilon \epsilon_o A}{d'} \quad (3.4)$$

where, ϵ and ϵ_o are the dielectric constant or permittivity of the capacitor, and the permittivity of free space (8.854×10^{-12} F/m) respectively, A is the conducting electrodes' area and d' is the thickness of the disc capacitor. Dielectric constant is the ratio of the amount of electrical energy stored in an insulator relative to vacuum, when the dielectric is subjected to an electric field.

For the electrical properties measurement both the surfaces of the sintered pellets were pasted by silver and cured at a temperature of 650°C in an oven for 2 hours. Care should be taken that the two faces of the pellet should not be conducting.

The capacitance (C) of this disc capacitor and dielectric loss factor ($\tan \delta$) of the same were measured using a Solatron 1260 Impedance/Gain-Phase Analyzer with a frequency ranges from 100 to 1000000 HZ.

3.4.4.2 Polarization with electric field study.

The P-E loop measurement was done in a P-E loop tracer (Marine India Electronics). The pellets were electroded with silver paint and cured at 650°C for 2h.

Materials exhibiting ferroelectricity should be of solids composed of crystallites and also possess reversible spontaneous polarization which can be reversed by the application of an external electric field. Hysteresis is one of the prominent features of ferroelectricity exhibiting a non-linear relationship between the polarization P and applied field E .

CHAPTER 4

RESULTS AND DISCUSSIONS

4.1 Density measurement.

The Bulk densities and apparent porosity of each sample sintered at different temperatures are measured by the Archimedes principle and depicted in the Table 4.1,4.2 and 4.3

Table 3 Comparison of AP and BD values of pallets sintered at 1050⁰c for batch 1

Sample	Dry wt(gm.)	Soaked wt.(gm)	Suspended wt(gm.)	Aparantporosity(%)	Bulk density
BaBi ₂ Nb ₂ O ₉ (pure)	0.859	0.8853	0.7312	17	5.5
BaBi ₂ Nb ₂ O ₉ (75%)- SrBi ₂ Nb ₂ O ₉ (25%)	0.847	0.9034	0.7209	30	4.6
BaBi ₂ Nb ₂ O ₉ (50%)- SrBi ₂ Nb ₂ O ₉ (50%)	1.632	1.7371	1.3991	31	4.8
BaBi ₂ Nb ₂ O ₉ (50%)- SrBi ₂ Nb ₂ O ₉ (50%)	0.845	0.8581	0.7170	9.2	5.9
SrBi ₂ Nb ₂ O ₉ (pure)	1.0384	1.0405	0.8957	1.4	7.1

Table 4 Comparison of AP and BD values of pallets sintered at 1100⁰c for batch 2

Sample	Dry wt(gm.)	Soaked wt.(gm(Suspended wt(gm.)	Aparantporosity(%)	Bulk density
SrBi ₂ Nb ₂ O ₉ (pure)	0.777	0.6675	0.7878	8.9	6.4
BaBi ₂ Nb ₂ O ₉ (75%)- SrBi ₂ Nb ₂ O ₉ (25%)	0.621	0.5383	0.6212	0.2	7.3
BaBi ₂ Nb ₂ O ₉ (50%)- SrBi ₂ Nb ₂ O ₉ (50%)	0.662	0.5640	0.6694	7.0	6.3
BaBi ₂ Nb ₂ O ₉ (50%)- SrBi ₂ Nb ₂ O ₉ (50%)	0.777	0.6857	0.7891	11.7	7.3
BaBi ₂ Nb ₂ O ₉ (pure)	0.961	0.8329	0.9260	0.7	7.4

Table 5 Comparison of AP and BD values of pallets sintered at 1100⁰c for batch 3

Sample	Dry wt(gm.)	Soaked wt.(gm(Suspended wt(gm.)	Aparantporosity(%)	Bulk density
SrBi ₂ Nb ₂ O ₉ (pure)	0.6685	0.6693	0.5694	0.8	6.69
BaBi ₂ Nb ₂ O ₉ (75%)- SrBi ₂ Nb ₂ O ₉ (25%)	0.8090	0.8153	0.6629	4.1	5.31
BaBi ₂ Nb ₂ O ₉ (50%)- SrBi ₂ Nb ₂ O ₉ (50%)	0.8508	0.8570	0.7147	4.3	5.98
BaBi ₂ Nb ₂ O ₉ (50%)- SrBi ₂ Nb ₂ O ₉ (50%)	0.8596	0.8605	0.7419	0.7	7.2
BaBi ₂ Nb ₂ O ₉ (pure)	0.9669	0.9672	0.8274	0.2	6.9

From the above data of density calculation at 2 diffarent temperature of 1050⁰c and 1100⁰c is mentioned and it is concluded that the density is better at the sintering temperature of 1100⁰c than 1050⁰c. so the characterization of the materials were done after sintering at 1100⁰c.

4.2 Phase formation behaviour

The phase formation behavior is studied by XRD analysis of the corresponding materials by compairing the obtained peaks of the XRD graph with the JCPDF file of that composition by the help of the Xpert Highscore software. Fig.3 shows the XRD pattern for all compositions. From the top to bottom of the graph represent the XRD pattern of the pure SBN, 75% SBN-25%BBN, 50% SBN-50% BBN, 25% SBN-75%BBN, and pure BBN respectively and all the graphs were matched with JCPDF standard files.

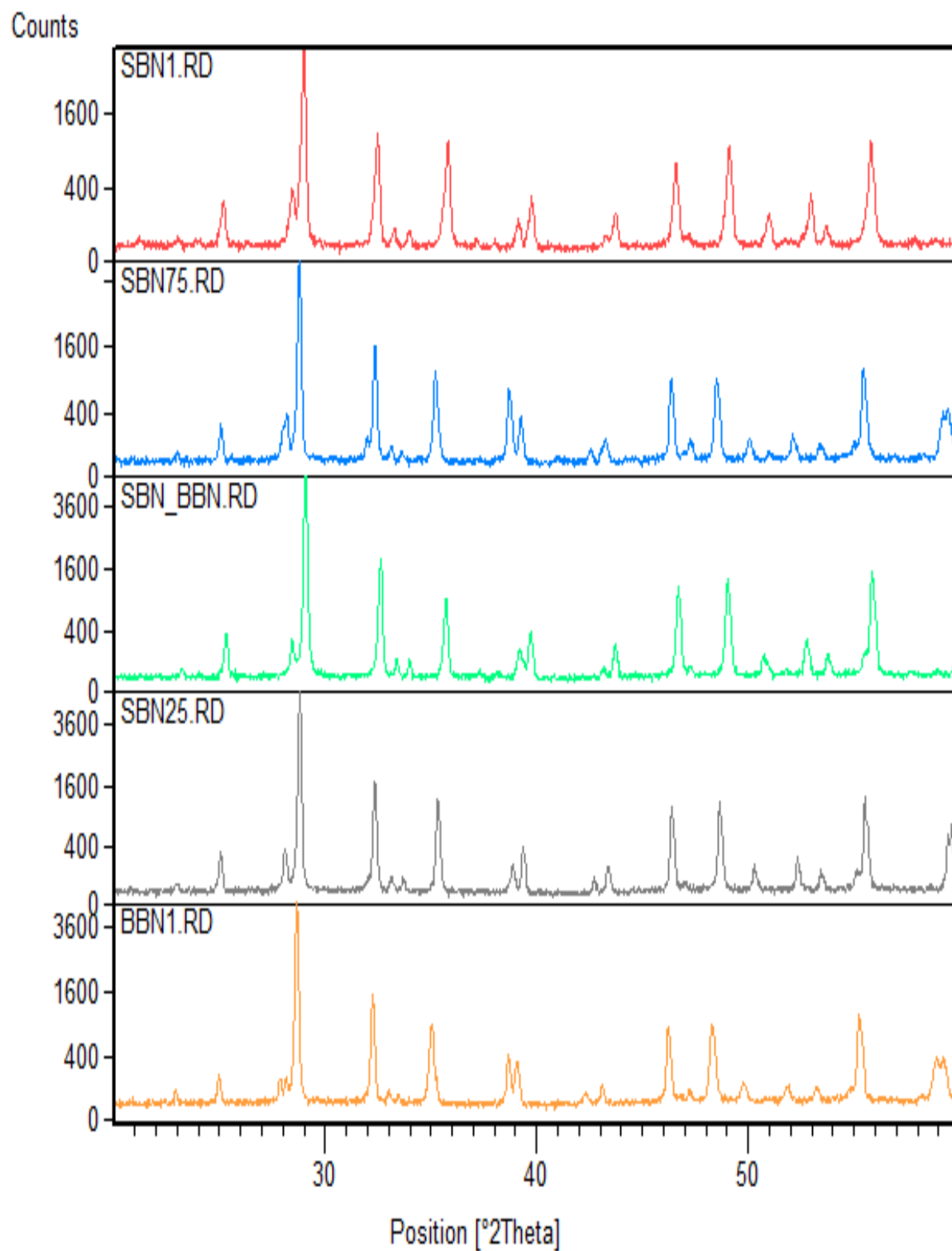


Figure 3 XRD pattern of samples sintered at 1100⁰c for a holding time of 4 hours.

From the values of (h,k,l) and d obtained from the corresponding patterns, the values of lattice parameters that is the value of a , b and c were calculated and plotted on a graph and represented on the Figure 4. It depict that the values of c is much higher than the values of a and b which implies the crystal structure is anisotropic.

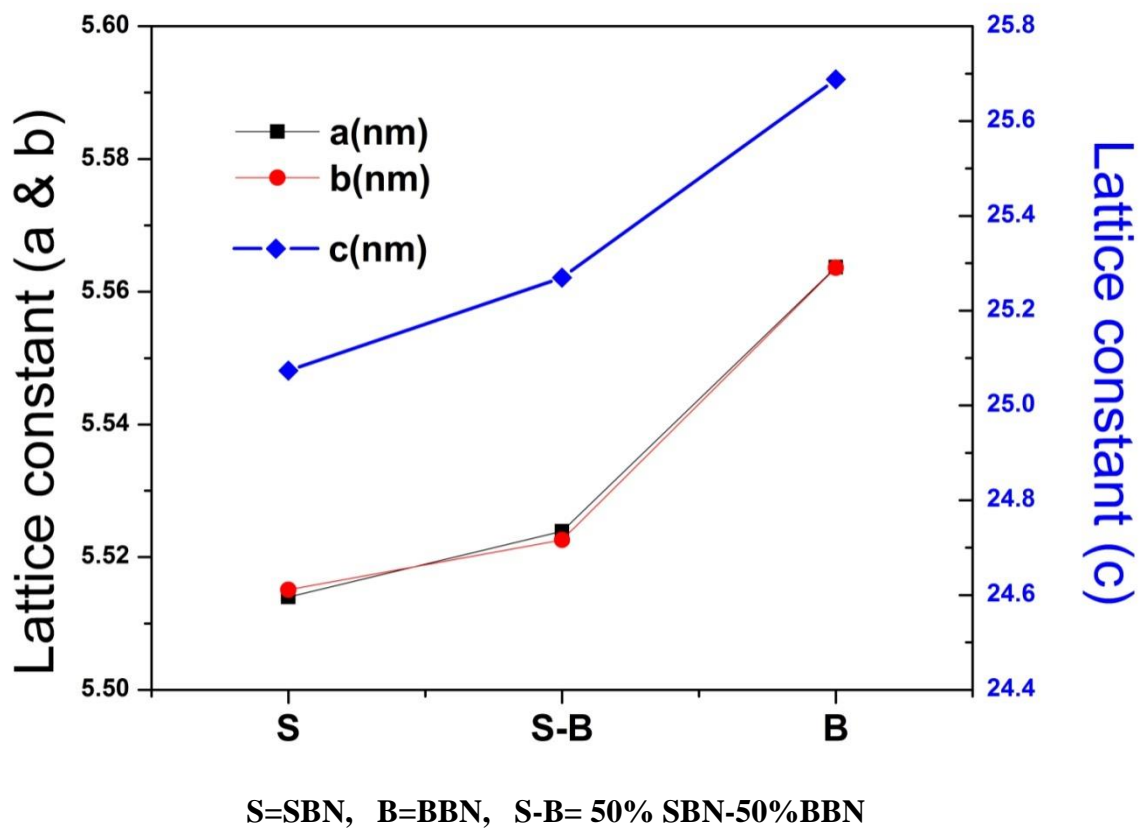


Fig. 4 Lattice parameter values comparison of SBN , BBN and their 1:1 solid solutions

4.3 Microstructural analysis

The SEM Figures (Fig. 5) of materials shows that the pure BBN has coarse grains whereas the pure SBN grains has elongated structures and according to the percentage of the two materials the grains of the compositions varies. That means for 75% SBN has more elongated grains whereas the 25% SBN contain has coarser grains.

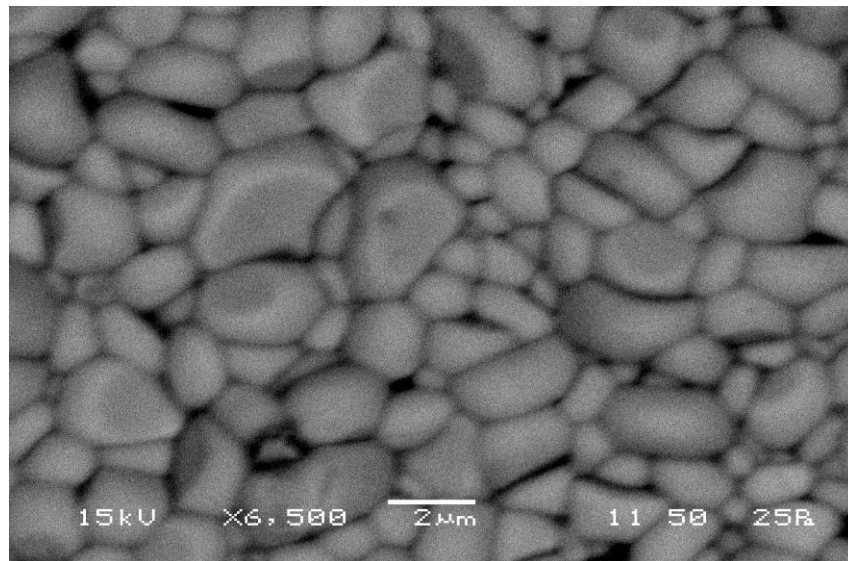


Figure 5 (a) Micro structure of pure BBN

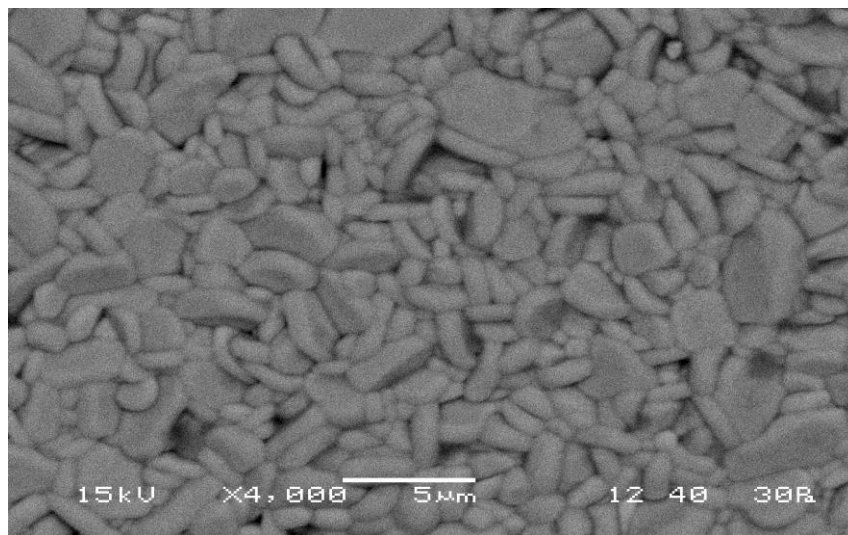


Figure 5(b) Micro structure of pure SBN

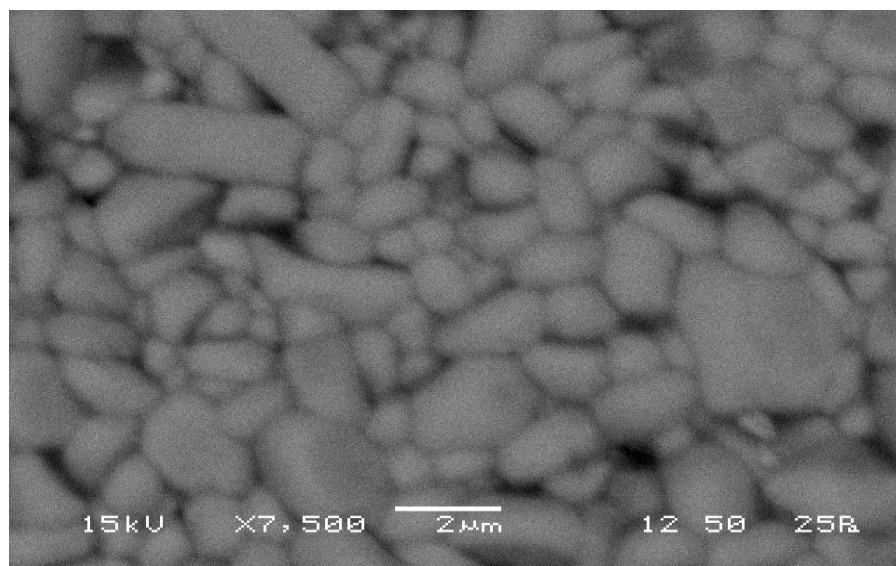


Figure 5(c) Micro structure of 25% SBN-75%BBN

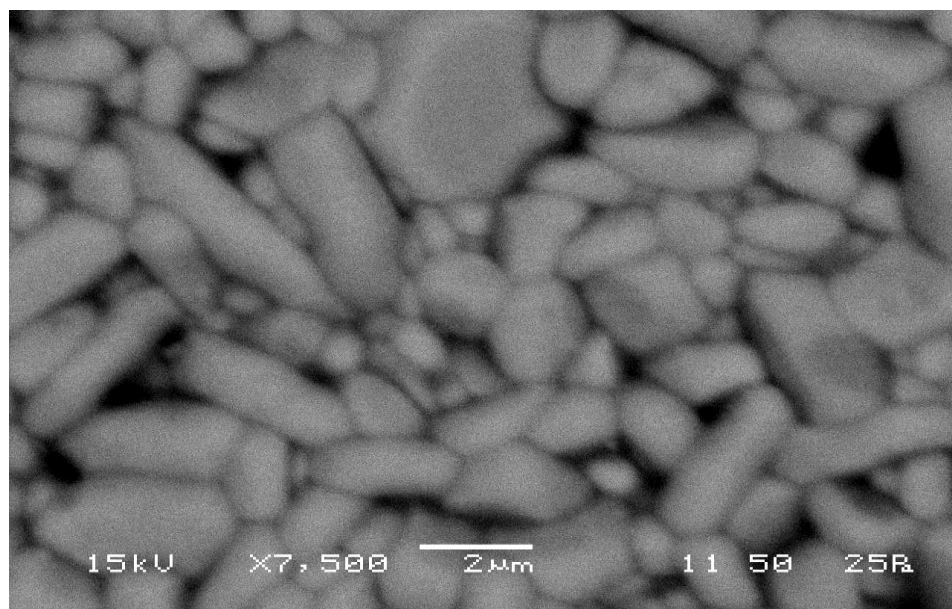


Figure 5(d) Micro structure of 50% SBN-50% BBN

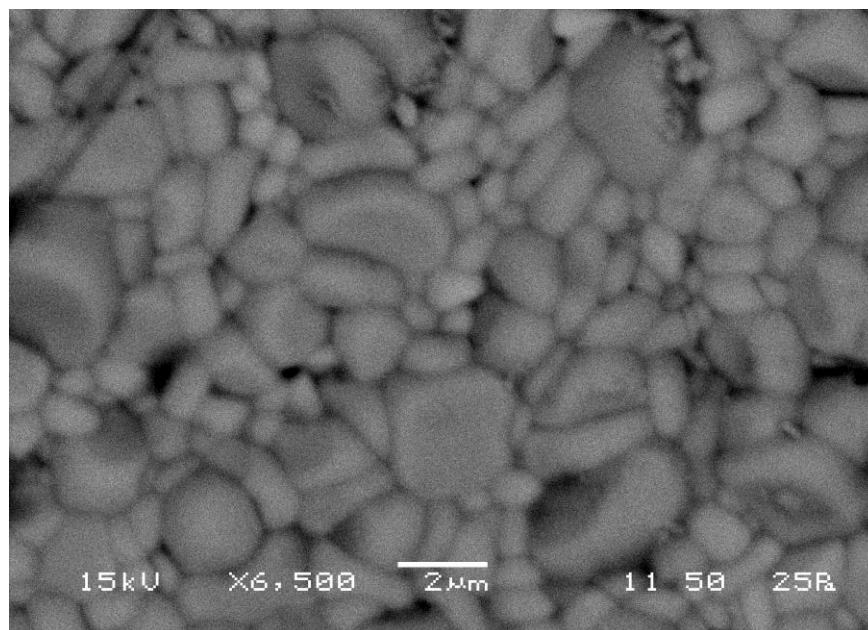


Figure 5(e) Micro structure of 75% SBN-25%BBN

4.4 Electrical properties

The Figure 6 depicts the relationship of relative permittivity with respect to frequency. It is concluded from the above graph is that the SBN has a lower permittivity value than BBN and the composition of 75% SBN and 25% BBN has a highest value amongst the all.

Fig 7 shows the frequency dependency of (loss factor) $\tan\delta$. It is concluded from the Figure 7 is that the loss of SBN is lowest and the loss of BBN is highest amongst all compound. A special characteristic is observed for the 50-50 solid solution composition of SBN and BBN, which has also very low loss factor frequency higher than 10 kHz. The low loss factor is suitable for better ferroelectric application of the materials.

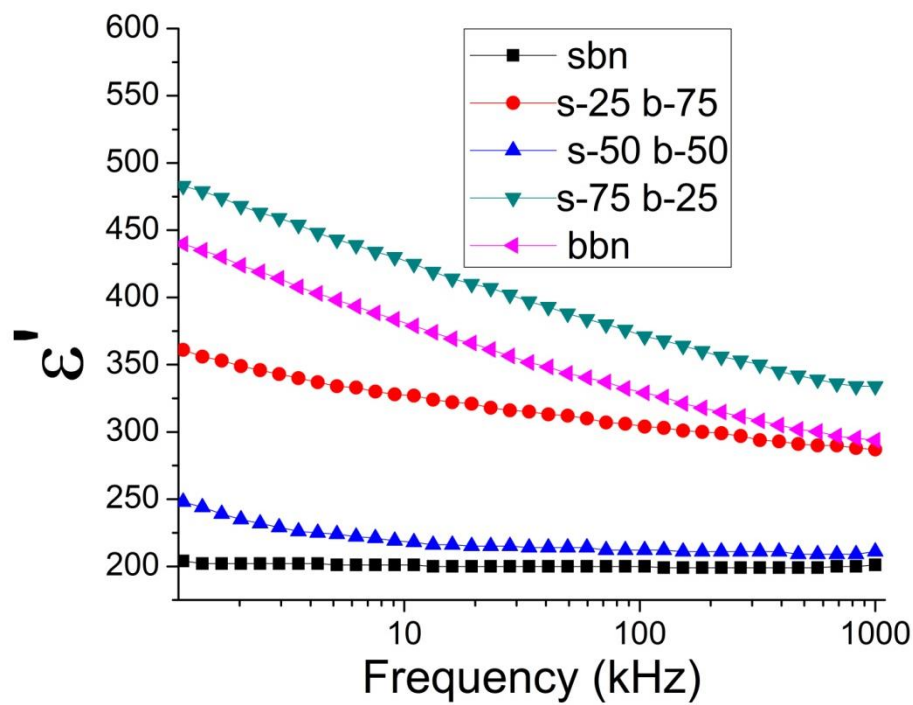


Figure 6 Permittivity vs frequency plot of samples

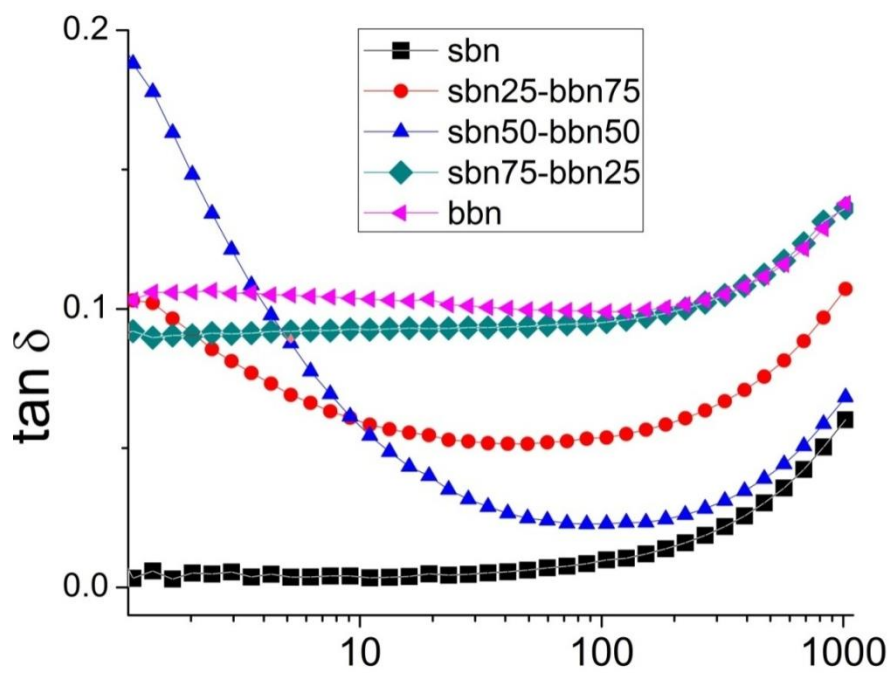


Figure 7 Frequency vs loss factor plot of samples

The Figure 4.4.3 is the relationship of the polarization vs applied electric field. On the above graph it is obvious that the blue colour opal has a wider area than all the others materials .a wider area in the P-E loop graph implies that it has a higher remnant polarization and also a high value of coercive field which is the required properties for a good ferroelectric material.

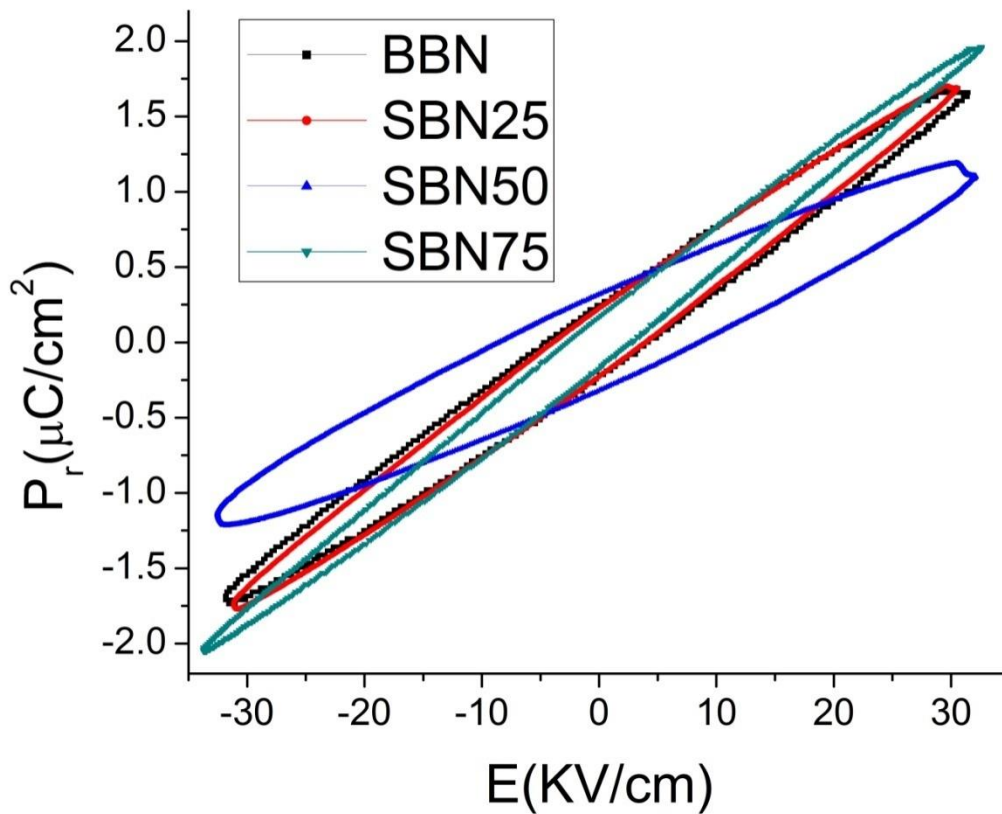


Figure 8 Polarisation vs electric field plot

CHAPTER 5

CONCLUSION

Conclusion

Substituted $\text{Ba}_{1-x}\text{Sr}_x\text{Bi}_2\text{Nb}_2\text{O}_9$ with $x = 0.25, 0.50, 0.75, 1$ were synthesized through solid oxide reaction route. Pure phase 3- layer BLSF compounds and there solid solution were formed at a calcination temperature of 900°C . The powders were sintered at 1050°C and 1100°C .

$\text{BaBi}_2\text{Nb}_2\text{O}_9$ ceramics has a better sinterability than $\text{SrBi}_2\text{Nb}_2\text{O}_9$ ceramics. Their 50-50 solid solution also had a good sinterability. The lattice parameters of the ceramics continuously decrease with the substitutions of Sr on Ba due t the lower ionic radius of Sr. $\text{BaBi}_2\text{Nb}_2\text{O}_9$ ceramic showed more circular grain with contrast to more elongated plate like grain of $\text{SrBi}_2\text{Nb}_2\text{O}_9$ ceramic.

The dielectric permittivity of $\text{BaBi}_2\text{Nb}_2\text{O}_9$ ceramic and 75% $\text{SrBi}_2\text{Nb}_2\text{O}_9$ – 25% $\text{BaBi}_2\text{Nb}_2\text{O}_9$ ceramic showed highest dielectric permittivity due to their very high density ; whereas $\text{SrBi}_2\text{Nb}_2\text{O}_9$ ceramic showed lowest loss factor due to its lower bulk density. It is interesting to note that 50-50 solid solution of $\text{BaBi}_2\text{Nb}_2\text{O}_9$ and $\text{SrBi}_2\text{Nb}_2\text{O}_9$ ceramics had a higher remnant polarization and coercive field. So this composition could be a better piezoelectric material.

CHAPTER 6

REFERENCES

References

1. E. C. Subbarao, J. Am. Ceram. Soc., 45 (1962) 564.
2. E. C. Subbarao, J. Am. Ceram. Soc., 45 (1962) 166.
3. B. Aurivillius, P. H. Fang, Phys. Rev., 126 (1962) 893.
4. H.N. Lee, D. Hesse, N. Zakharov, U. Gosele, Science 296 (2002) 2006.
5. C.A. Paz de Araujo, J.D. Cuchiaro, L.D. McMillan, M.C. Scott, J.F. Scott, Nature 374 (1994).
6. B.H. Park, B.S. Kang, S.D. Bu, T.W. Noh, J. Lee, W. Jo, Nature (London) 401 (1999) 682.
7. S. T. Jhang, C.S. Xiao, A.A. Fang, B. Yang, B. Sun, Y. F. Chen, Z.G. Liu, Appl. Phys. Lett. 76 (2000) 3112.
8. Y. Noguchi, M. Miyayama, T. Kudo, Appl. Phys. Lett. 77 (2000) 3639.
9. S. Horiuchi, H. Nagata, T. Takenaka, Ferroelectrics, 324 (2005) 3-9.
10. S.P. Gaikwada, H.S. Potdara, Violet Samuelb, V. Ravi, Ceramics International 31 (2005) 379–381
11. C. Karthik, K.B.R. Varma, Materials Science and Engineering B 129 (2006) 245–250
12. M. Adamczyk, L. Kozielska, M. Pilchb, n, M. Pawe"czykc, A. Soszyn´ski, Ceramics International 39 (2013) 4589–4595
13. Puja Goel, K.L. Yadav, Physica B 382 (2006) 245–251
14. Pinyang Fang a,† , Huiqing Fan b, Zengzhe Xi a, Weixing Chen a, Shanchuan Chen a, Wei Long a, Xiao, Journal of Alloys and Compounds 550 (2013) 335–338